

MULTIRATE SIGNAL PROCESSING AND ITS APPLICATIONS

Author: Roday Vikram Singh
Roll no.: 03307062
Supervisor: Prof. V.M. Gadre

Abstract

Wavelets are implemented using Multirate signals. Wavelets are functions defined over a finite interval and having an average value of zero. They are compactly supported. The signal power at large scales corresponds to that at low frequencies in the fourier transform; the power at small scales corresponds to that at high frequencies in the fourier transform.

The report describes two applications of wavelets. The first application is a wavelet transform domain filter which removes noise from a signal while preserving edges in it. It uses direct spatial correlation of wavelet transform contents at several adjacent scales to accurately determine locations of edges. The second is discriminating between internal faults and inrush currents in power transformers accurately.

Introduction

The motivation in studying wavelet transforms was provided by the fact that signals can be modeled suitably by combining translations and dilations of a simple, oscillatory function of finite duration called a wavelet. Wavelet transforms are found in work done in the field of seismic signals, quantum mechanics, modeling multiscale phenomenon, solution of partial differential equation, statistics, communications and signal and image processing. In signal and image processing they are useful in many areas including filtering of noisy data, compression, fingerprint compression, edge detection, etc.

Consider a real or complex-value continuous-time function $\psi(t)$ with the following properties:

- 1) The function integrates to zero

$$\text{ie } \int_{-\infty}^{\infty} \psi(t) dt = 0$$

- 2) It is square integrable or, equivalently, has finite energy:

$$\text{ie } \int_{-\infty}^{\infty} |\psi(t)|^2 dt < \infty$$

- 3) It satisfies the admissibility condition ie

$$0 < \int_{-\infty}^{\infty} \frac{|\psi(\omega)|^2}{|\omega|} d\omega < \infty$$

The function $\psi(t)$ is a mother wavelet or wavelet if it satisfies these properties [1]. It should be noted that properties (1) and (2) are sufficient to call the function as a wavelet. The property (3) is useful in formulating a simple inverse transform.

Property 1 is suggestive of a function that is oscillatory or that has a wavy appearance (A function does not necessarily have to oscillate to satisfy this property). Property 2 implies that

most of the energy in $\psi(t)$ is confined to a finite duration. Thus, in contrast to a sinusoidal function, it is a “small wave” or a wavelet. Properties 1 and 2 are easily satisfied and there is an infinity of functions that quantify as mother wavelets. Figures below shows plot of various wavelets.

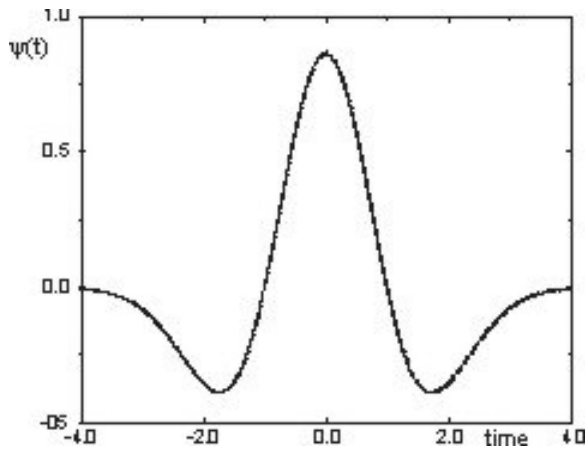


figure 1 Mexican hat wavelet [1]

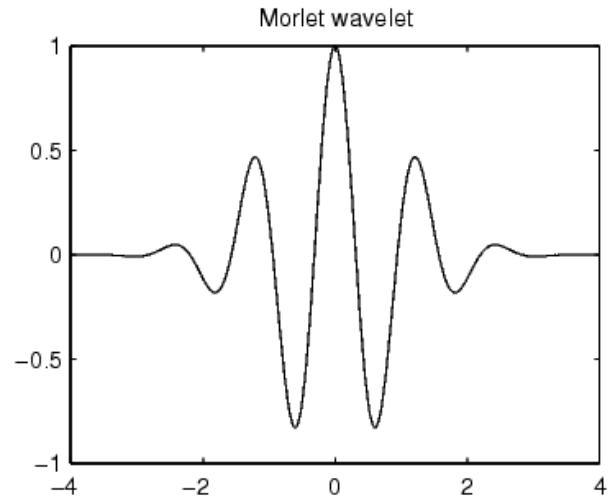


figure 2 Morlet wavelet [1]

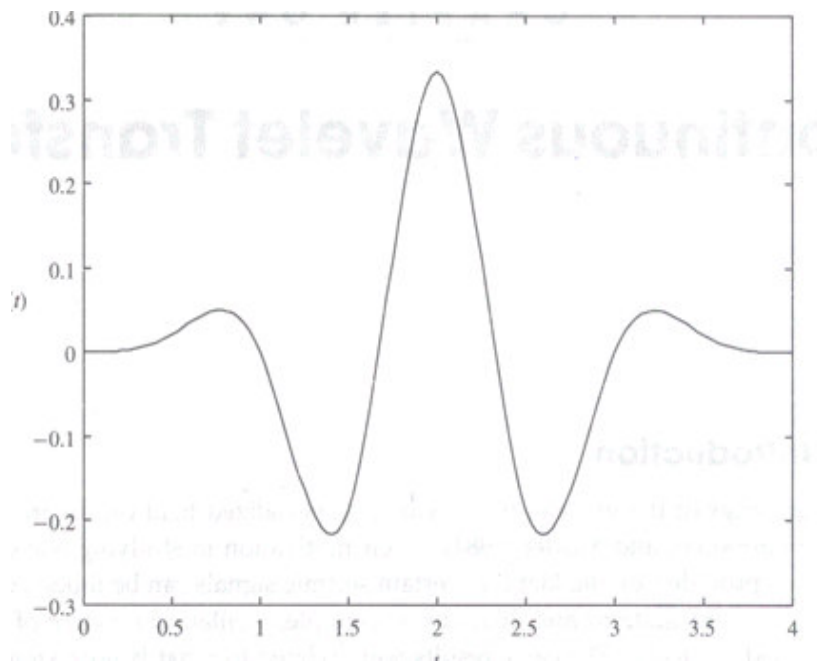


figure 3 Cubic B-spline wavelet [1]

Cubic B-spline wavelet is compactly supported ie the entire wavelet has a finite duration: $0 \leq t \leq 4$ sec.

Continuous time wavelet transform (CWT):

Let $f(t)$ be any square integrable function. The continuous-time wavelet transform of $f(t)$ with respect to a wavelet $\psi(t)$ is defined as [1]

$$W(a,b) = \int_{-\infty}^{\infty} f(t) \frac{1}{\sqrt{|a|}} \psi^* \left(\frac{t-b}{a} \right) dt$$

Where a and b are real and $*$ denotes complex conjugation. Thus, wavelet transform is a function of two variables. Observe that both $f(t)$ and $\psi(t)$ belong to $L^2(\mathbb{R})$, the set of energy signals.

The above equation can be written in more compact form by defining $\psi_{a,b}(t) = \frac{1}{\sqrt{|a|}} \psi \left(\frac{t-b}{a} \right)$

Therefore,

$$W(a,b) = \int_{-\infty}^{\infty} f(t) \psi_{a,b}^*(t) dt$$

Notice that

$$\psi_{1,0}(t) = \psi(t)$$

The normalizing factor of $1/\sqrt{|a|}$ ensures that the energy stays the same for all a and b ; ie

$$\int_{-\infty}^{\infty} |\psi_{a,b}(t)|^2 dt = \int_{-\infty}^{\infty} |\psi(t)|^2 dt$$

for all a and b .

For any given value of a , the function $\psi_{a,b}(t)$ is a shift of $\psi_{a,0}(t)$ by an amount b along the time axis. Thus, the variable b represents time shift or translation. Since, the variable a determines the amount of time scaling or dilation, it is referred to as the scale or dilation variable. If $a > 1$, there is a stretching of $\psi(t)$ along the time axis, whereas if

$0 < a < 1$, there is a contraction of $\psi(t)$. Negative values of a result in a time reversal in combination with dilation. Since the CWT is generated using dilates and translates of the single function $\psi(t)$, the wavelet for the transform is referred to as the mother wavelet.

If the mother wavelet satisfies the admissibility condition (property 3), then inverse CWT exists and is defined as

$$f(t) = \frac{1}{C} \int_{a=-\infty}^{\infty} \int_{b=-\infty}^{\infty} \frac{1}{|a|^2} W(a,b) \psi_{a,b}(t) da db$$

where $C = \int_{-\infty}^{\infty} \frac{|\psi(t)|^2}{|t|} dt$

Wavelet transform provides a weighting function for synthesizing a given function $f(t)$ from the translates and dilates of the mother wavelet much as the Fourier transform provides a weighting function for synthesizing a function from sine and cosine functions.

Discrete Wavelet Transform (DWT)

CWT maps 1-D function $f(t)$ to a function $W(a,b)$ of two continuous real variable a and b . The region of support of $W(a,b)$ is defined as the set of ordered pairs (a,b) for which $W(a,b) \neq 0$. The region of support of CWT is unbounded. CWT provides a redundant representation of the signal in the sense that the entire support of $W(a,b)$ need not be used to recover $f(t)$ [1].

We look into a representation of the form

$$f(t) = \sum_{k=-\infty}^{\infty} \sum_{l=-\infty}^{\infty} d(k,l) 2^{-k/2} \psi(2^{-k}t - l)$$

which uses discrete values for dilations and translations parameters. The dilation take the values of the form $a = 2^k$ where k is an integer. At any dilation 2^k , the translation parameter takes values of the form $2^k l$ where l is again an integer. The values $d(k,l)$ are related to values of the wavelet transform $W(a,b) = \mathcal{W}[f(t)]$ at $a = 2^k$ and $b = 2^k l$ and is referred to as the Discrete Wavelet Transform (DWT).

DWT of a signal $x(t)$ with respect to a wavelet $h(t)$ is given by

$$X_{DWT}(m, k) = 2^{-m/2} \int_{-\infty}^{\infty} x(t) h(kT - 2^{-k}t) dt$$

As can be clearly observed, DWT is a mapping from a one dimensional signal $x(t)$ to a two dimensional sequence $X_{DWT}(m, k)$ as shown in figure 4. The index m in essence corresponds to the center frequency of the bandpass analysis filters, and corresponds to a non-uniform partitioning of the frequency axis. The center frequency is halved each time m is increased by 1. Furthermore, since the filters are sampled increasingly slower with larger m , the index k corresponds to the multiple of the sampling period $2^k T$.

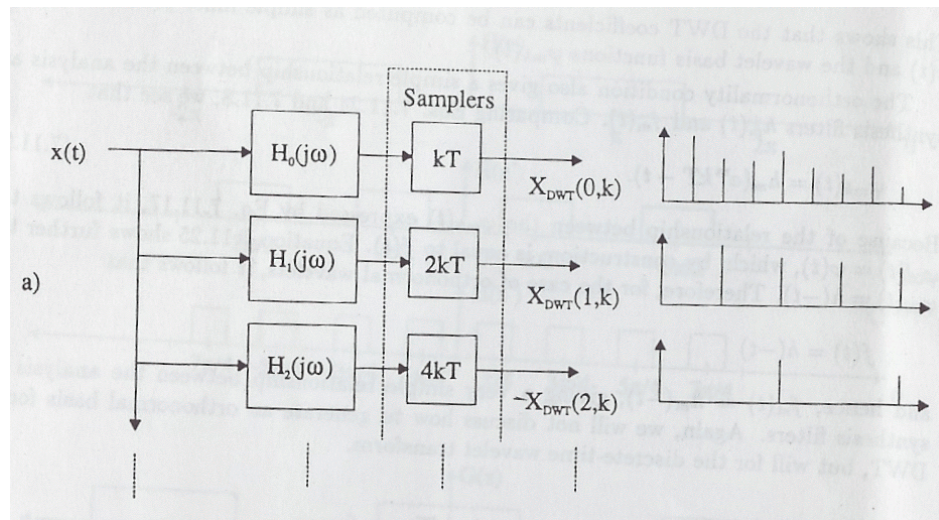


figure 4 Schematic illustration of the DWT

Figure 4 gives a schematic depiction of how the DWT can be computed using an analysis filter bank. The original signal $x(t)$ can be recovered from the DWT, by designing a synthesis filter bank with inputs equal to the DWT coefficients. A synthesis filter bank is shown in fig 5 where the synthesis filters are given by $F_m(j\omega)$.

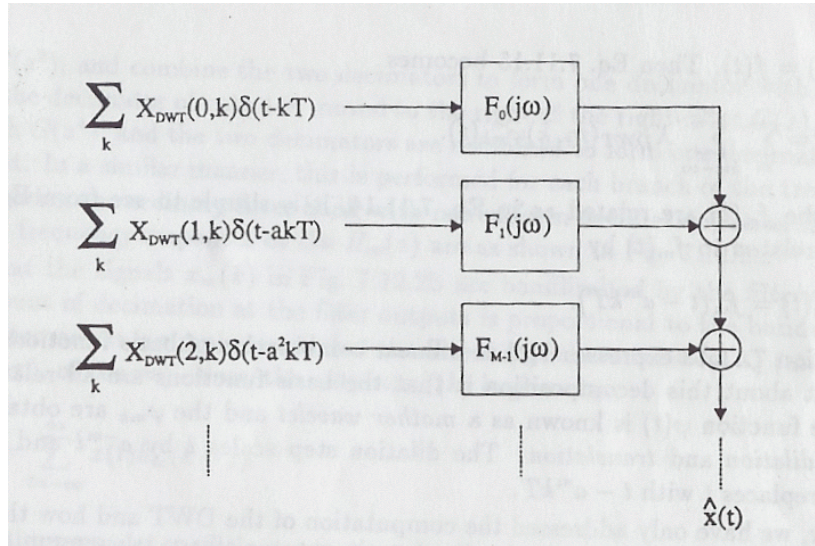


figure 5 Synthesis bank to reconstruct $x(t)$ from $X_{DWT}(m, k)$

Wavelet transform domain filter

Fourier transform domain filters used in signal and image processing involve a tradeoff between the signal-to-noise ratio(SNR) and the spatial resolution of the signal/image processed. Low-pass filters will not only smooth away noise but will also blur edges in signals and images; high-pass filters can make the edges even sharper and improve the spatial resolution but will also amplify the noisy background. We will study spatial filters in the wavelet transform domain as an alternative to fourier transform domain filter. This filter can be seen as a low-pass filter that passes selected high-frequency data. The high-frequency data passed is that which occurs at position where edges are identified.

The signal power at large scales corresponds to that at low frequencies in the fourier transform; the power at small scales corresponds to that at high frequencies in the fourier transform [1]. The filter pass essentially all the signal at large scales. The signal at small scales is passed if it is around an identified edge; it is eliminated as noise if it is not around an identified edge. Because most noise power is confined to small scales, the reduction of signal at small scales reduces noise preferentially. However, to keep edges sharp, small-scale information is required. By passing small scale data around identified edges, noise is reduced, and the identified edges stay sharp. The key to this technique is to identify edges. Edges are identified as features that have signal peaks across many scales. An edge occur at a position where there are maxima in the nonorthogonal wavelet transform at several adjacent scales [2]. Direct spatial correlations of wavelet transform at different scales are used to identify the edges; the small scale data is passed at positions where the correlation is large and suppressed if the correlation is small.

We use the direct multiplication of wavelet transform data at adjacent scales to distinguish important edges from noise and accomplish the task of removing the noise from signal. This approach is more straightforward, easier to implement, and significantly more robust.

Sharp edges have large signal over many wavelet scales, and noise dies out swiftly with increasing scale. Direct spatial correlation $\text{Cor } r_l(m,n)$ of wavelet transform contents at several adjacent scales accurately determine the locations of edges or other significant features.

$$\text{Cor } r_l(m,n) = \prod_{i=0}^{l-1} W(m+i, N) \quad n=1,2,\dots,N$$

Where l is the number of scale involved in the direct multiplication, $m < M-l+1$, and M is the total number of scales.

Figure 6 shows a simulated 1-D data set of 256 points and its discrete, dyadic wavelet transform at all eight scales. In the simulated data there are two small “bumps” on top of a large boxcar and added Gaussian distributed white noise. The SNR of the data is about 18db.

Figure 7 demonstrates the effect of this wavelet filter on the smallest (first) scale of the wavelet transform of the signal shown in figure 6. Figure 7(b) gives the direct multiplication of the wavelet transform contents at the first two smallest scales $\text{cor } r_2(1,n) = W(1,n)W(2,n)$. Note that the two edges of the large boxcar in the original data set show up much sharper and stronger in $\text{cor } r_2(1,n)$ than they appear in $W(1,n)$. Furthermore, one may observe that they are much larger in $\text{cor } r_2(1,n)$ than the edges of the two small bumps and noisy background.

First, the power of the $\text{cor } r_2(1,n)$ data is rescaled to that of the $W(1,n)$ data. The most important edges (two major edges in fig 7) are identified in $W(1,n)$ and $\text{cor } r_2(1,n)$ by comparing the absolute values of $\text{cor } r_2(1,n)$ and $W(1,n)$. An edge is identified at any position n for which $|\text{cor } r_2(1,n)| > |W(1,n)|$. This edge position and its corresponding value $W(1,n)$ are stored. Finally, all the edges identified in this way are extracted from $\text{cor } r_2(1,n)$ and $W(1,n)$ by resetting the values of these signals to 0's at the positions identified. We refer to the remainder of the data points in $W(1,n)$ and $\text{cor } r_2(1,n)$ after the first round of data extraction as $W'(1,n)$ and $\text{corr}'_2(1,n)$. By rescaling the power of $\text{corr}'_2(1,n)$ to that of $W'(1,n)$ and comparing their absolute values, the next most significant edges (edges of two small bumps in fig 7) are extracted from $W(1,n)$ and $\text{cor } r_2(1,n)$. This procedure of power normalization, data value comparison and edge information extraction can be iterated many times until the power of the unextracted data points in $W(1,n)$ is nearly equal to some reference noise power at the first wavelet scale. In digital image processing, one can often use the background noise as the dark regions (signal-free) near the boundaries of an image as the reference noise.

All the edge information in the original data that is extracted from $W(1,n)$ during this iteration process is kept in a data vector $W_{new}(1,n)$. By replacing $W(1,n)$ with $W_{new}(1,n)$, we can have a new and spatially filtered first scale wavelet transform data where most of the noise is removed and most of the original edges are preserved. By repeating the procedure at every resolution scale, we can acquire all the spatially filtered wavelet transform data $W_{new}(m,n)$. The reconstruction from $W_{new}(m,n)$ through the inverse wavelet transform shown in fig 8 will yield the final filtered signal.

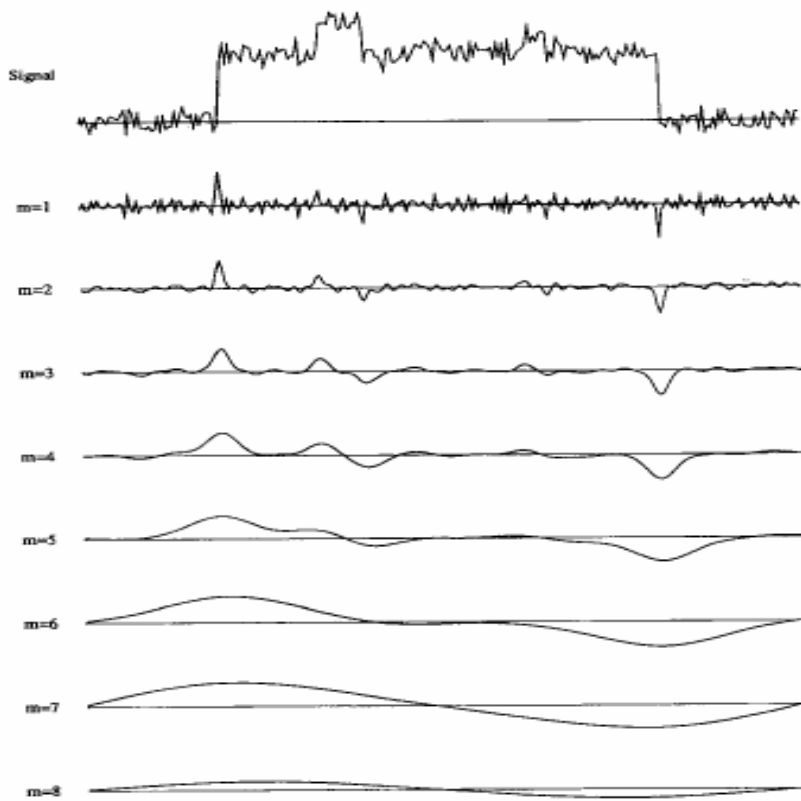


Figure 6 Simulated 1-D data of 256 points and its discrete dyadic transform [2]

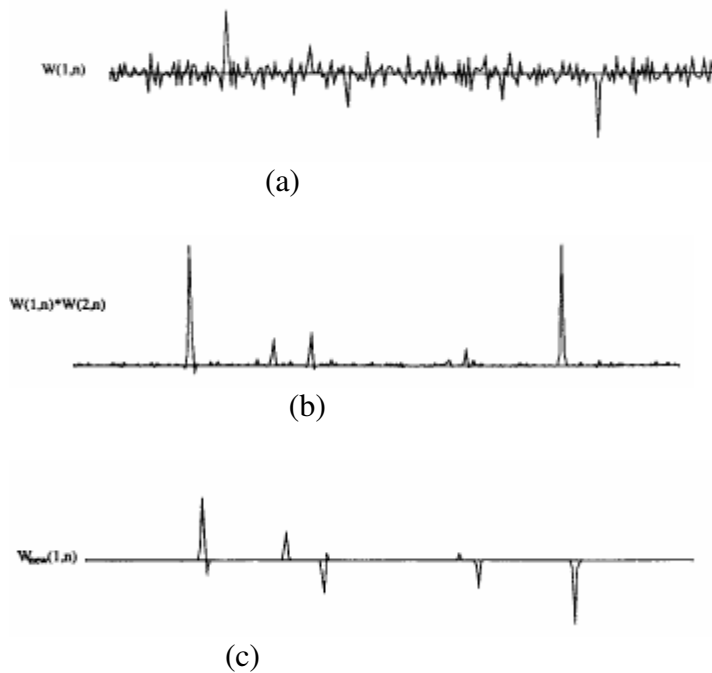


figure 7 Graphic illustration of noise filtration technique (a) first scale wavelet transform $W(1,n)$ before filtering; (b) Direct multiplication of $w(1,n)$ and $W(2,n)$; (c) $W_{new}(1,n)$ after filtering [2]

Figure 8 shows that the edges of the large boxcar and the higher bump remain as sharp after filtration as they were before filtration. Noise reduction is remarkable. It reduces from 18 to 26.3 dB.]

There is slight degradation in both the edges and the contrast of small features (ie the smaller bump in the simulated data). It is difficult for the filter to discriminate between noise the features that are the same size as the noise.

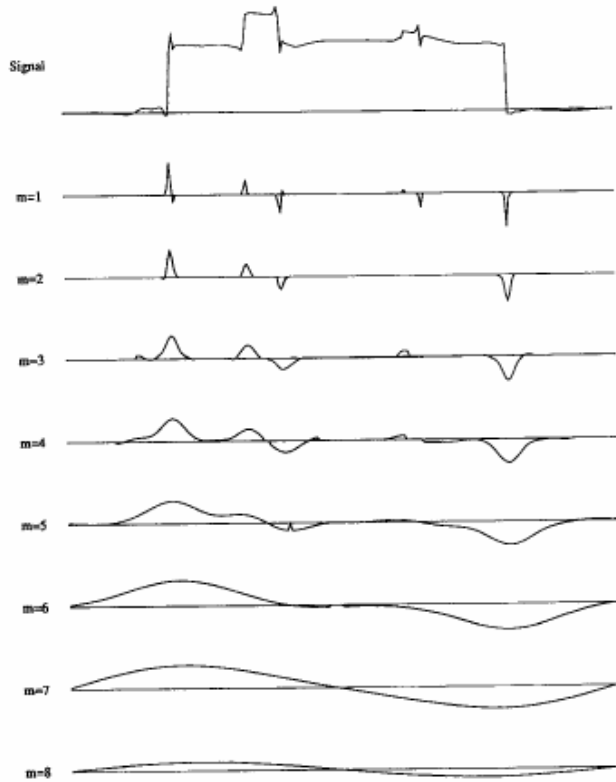


figure 8 1-D data and its discrete dyadic wavelet transform shown in fig. 6 after being processed with the wavelet domain filtering technique [2]

Transformer protection

Power transformer protection is of critical importance in power systems. Any power transformer protective scheme has to take into account the effect of magnetizing inrush currents. This is because the magnetizing inrush current, which occurs during the energisation of the transformer, sometimes results in 10 times full load currents and therefore can cause mal-operation of the relays [3]. Accurately discriminating between magnetizing inrush currents and internal faults is a key to solve this problem.

To avoid mal-operation due to inrush current, it is common practice to detect second harmonic component of current and block or restrain the differential protection of power transformer if it exceeds a certain value. However there are following drawbacks in this approach:

- 1) It has been reported that in certain cases, internal fault current might contain considerable amount of second harmonic content of measured current [4]. This may result in an operation with a time delay or non-operation of second harmonic restraint differential protection in case of internal faults or energization with internal faults.

2) On the other hand, it has been found that the second harmonic content in magnetizing inrush currents tends to be relatively small in modern power transformers because of improvements in power transformer core material (high quality, low loss core material) [5]. In some cases, the second harmonic components are not sufficient to restrain the relay adequately.

Here a simple decision making logic scheme based on wavelet transform for distinguishing internal faults from inrush currents is presented [3].

To demonstrate the effectiveness of the proposed scheme, a power transformer system 1 is studied. System 1 is a three-phase and two-winding 750 MVA, 27/420 kV, Dy11-connected, fiveleg core type power transformer in a double-end-fed power system network.

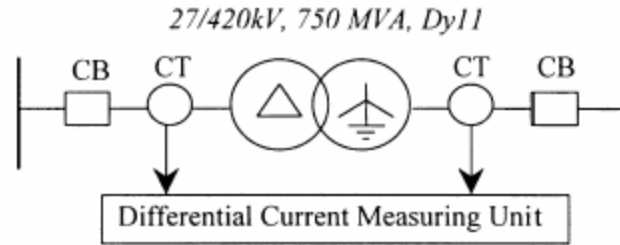


figure 9 systems simulated power transformer [3]

The simulations of these two power transformer systems have been carried out using the well-known EMTP software. The CT saturation has been taken into consideration.

In this study, the original differential current signal has been sampled at 25 kHz (the technique presented is based on employing the high-frequency phenomenon associated with transformer transients and hence necessitates the use of high sampling frequency of 25 kHz) and passed through a discrete wavelet transform (DWT), with the structure of Fig. 10, in which $x[n]$ is the original signal, $h[n]$ and $g[n]$ are low-pass and high-pass filters, respectively. At the first stage, an original signal is divided into two halves of the frequency bandwidth, and sent to both high-pass filter and low-pass filter. Then the output of low-pass filter is further cut in half of the frequency bandwidth, and sent to the second stage. The same procedure is performed until the signal is decomposed to a pre-defined certain level. Finally, we obtain a bunch of signals, which actually represent the same original signal, but all corresponding to different frequency bands. Thus, 5-detailed signals that contain a frequency band of 12.5–6.25 kHz at detail 1, 6.25–3.125 kHz at detail 2, 3.125–1.562 kHz at detail 3, 1.562kHz–781 Hz at detail 4 and 781–390 Hz at detail 5 as well as one approximate signal in the frequency band 390 Hz–DC level), are obtained.

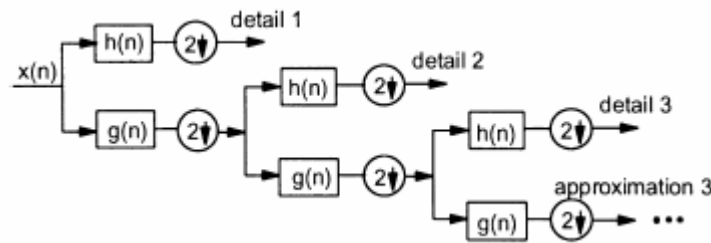


figure 10 Implementation of DWT [3]

Fig. 11(a) shows typical magnetising inrush current waveforms (i.e. the EMTP output signal), which corresponds to a , b and c three phase differential currents through the CT secondary sides in system 1. As can be seen, the current waveforms are distorted quite significantly; gaps appear over the times of the inrush currents. From Fig. 11(b)–(d), which correspond to a , b and c three phase wavelet signals at detail 1, it can be seen that there are four sharp spikes at the edges of gaps at which the inrush current suddenly changes from one state to

other different states. Another four sharp spikes are produced because the primary windings of the power transformer are connected in delta; for example the a -phase differential current is in fact the difference between the a phase magnetising inrush current and c -phase magnetizing inrush current. This gives rise to the non-smooth points in the current waveforms, which in turn cause sharp spikes to appear in the DWT of the current waveforms.

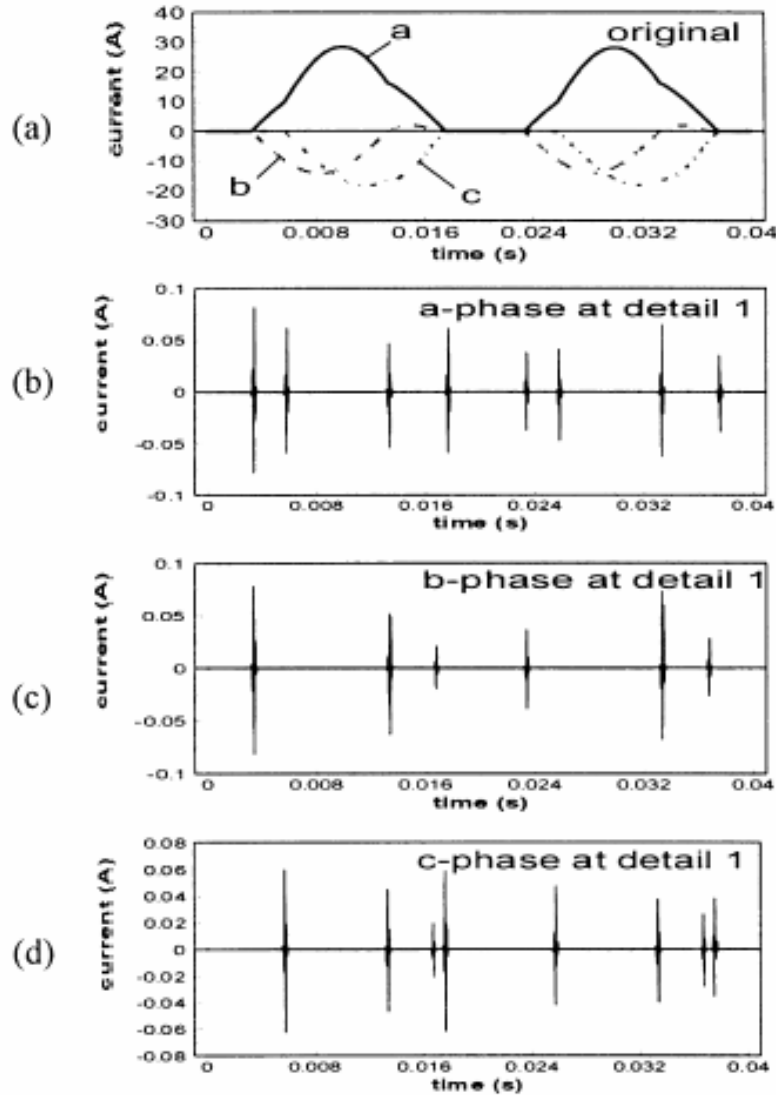


Fig. 11. Magnetising inrush currents in system 1: (a) original a , b and c three phase differential currents; (b) a -phase DWT at detail 1; (c) b -phase DWT at detail 1; and (d) c -phase DWT at detail 1 [3].

Fig. 12(a) shows an internal fault current, which corresponds to a , b and c three-phase differential currents through the CT secondary sides, under an a - b to earth fault on the high voltage side of the power transformer in system 1. It is apparent from Fig. 12(a) that there is a high-frequency distortion in the current waveforms. This is as a direct consequence of the effects of the distributed inductance and capacitance of the

transmission line. This can lead to a significant second harmonic in the internal fault , thereby posing difficulty in an accurate discrimination between magnetizing inrush and internal fault currents by the conventional protection method. As before, detail 1 is taken as the feature extraction shown in Fig. 12(b)–(d). From Fig. 12(b)–(d), we can see that there are several sharp spikes appearing from the inception time of the internal fault. The maximum value of the sharp spike appears at the beginning of the fault

Simulation studies shows that the wavelet transforms of magnetising inrush currents and internal fault currents have the following different features. For internal fault case, there are several sharp spikes appearing from the inception time of the internal fault. The maximum value of the sharp spike appears at the beginning of the fault. However, in marked contrast to the inrush current case, these sharp spikes rapidly decay to near zero within one cycle, whereas those sharp spikes under inrush current cases suffer from little attenuation during the entire inrush transient period, which can last from perhaps 10 cycle for small transformers to 1 min for large units . It is apparent that this difference can be used as the key feature to effectively distinguish internal faults from inrush currents

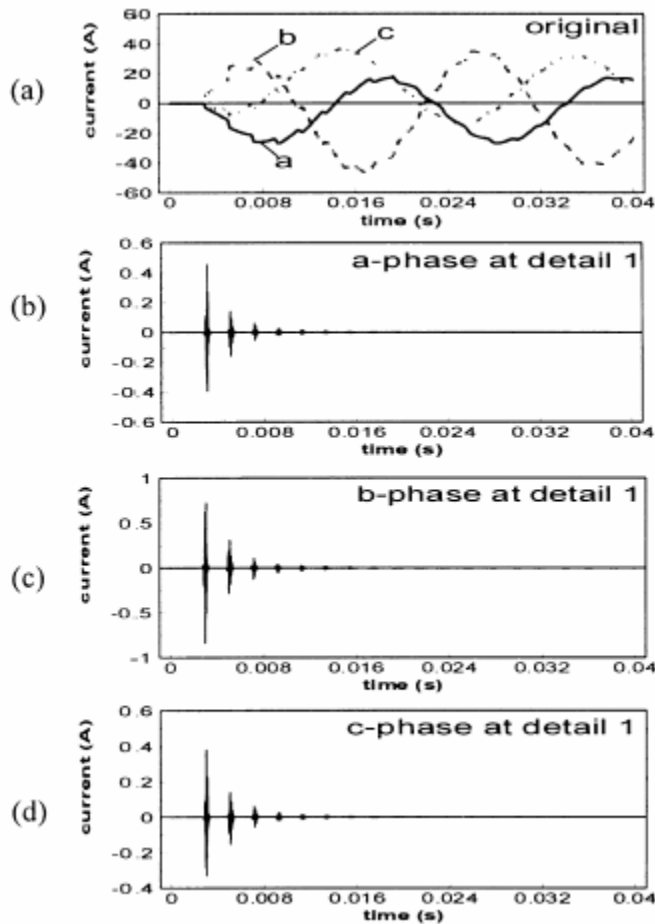


Fig. 12. Internal fault currents in system 1: (a) original *a*, *b* and *c* three phase differential currents; (b) *a*-phase DWT at detail 1; (c) *b*-phase DWT at detail 1; and (d) *c*-phase DWT at detail 1 [3].

The decision for discriminating between internal faults and inrush currents are made based on the extracted features that are quantified by a ratio in a certain wavelet component, which is given by the following equations.

$$I_{a-ratio} = \frac{I_{a-d1,max}^k}{I_{a-d1,max}}$$

$$I_{b-ratio} = \frac{I_{b-d1,max}^k}{I_{b-d1,max}}$$

$$I_{c-ratio} = \frac{I_{c-d1,max}^k}{I_{c-d1,max}}$$

where, $I_{a-d1,max}$, $I_{b-d1,max}$, $I_{c-d1,max}$ respectively, represent the maximum peak values of a -phase, b -phase, c -phase wavelet at detail 1 in the first window; $I_{a-d1,max}^k$, $I_{b-d1,max}^k$, $I_{c-d1,max}^k$; respectively, represent the maximum peak values of a -phase, b -phase, c -phase wavelet at detail 1 in the k th subsequent moving windows after the first window.

The decision for distinguishing between internal faults and inrush currents is made in terms of the ratio change in $I_{a-ratio}$, $I_{b-ratio}$ and $I_{c-ratio}$ in each moving window, which is given as follows:

If
 $(I_{a-ratio} > \varepsilon \text{ OR } I_{b-ratio} > \varepsilon \text{ OR } I_{c-ratio} > \varepsilon)$ then

“This is an inrush”

else

“This is an internal fault”

where, ε represents the predefined threshold

Conclusions

Wavelets are functions defined over a finite interval and having an average value of zero. The basic idea of the wavelet transform is to represent any arbitrary function as a superposition of a set of such wavelets or basis functions. These basis functions or baby wavelets are obtained from a single prototype wavelet called the mother wavelet, by dilations or contractions (scaling) and translations (shifts). CWT provides a redundant representation of signal. DWT is a nonredundant wavelet representation and can be implemented using multirate signals. Wavelet transform of $f(t)$ at small scale contains information about $f(t)$ at higher end of its frequency spectrum and vice-versa.

Results of wavelet transform domain filters using direct spatial correlation of edge detection data over several adjacent scales shows that noise is reduced very effectively with very little resolution loss; most sharp edges are preserved, and some of them are enhanced. However, features that are of the same size as noise are suppressed because they are not distinguished from the noise. Wavelet transform based method can effectively distinguish between internal faults and inrush currents in a power transformer.

References

- [1] R.M. Rao and A.S. Bopardikar, Wavelet Transforms-Introduction to Theory and Applications. Addison-Wesley, 2000.
- [2] Y. Xu, J.B. Weaver, D.M. Healy and J. Lu, “Wavelet Transform Domain Filters: A Spatially Selective Noise Filtration Technique,” IEEE Trans. Image Processing,

- [3] P.L. Mao and R.K Aggarwal, "A Wavelet Transform Based Decision Making Logic Method for Discrimination Between Internal Faults and Inrush Currents in Power Transformers," *Electrical Power and Energy Systems* 22, pp. 389-395, 2000.
- [4] Liu P, Malik OP, Chen D, Hope GS and Guo Y, "Improved Operation of Differential Protection of Power Transformers for Internal Faults," *IEEE Trans Power Delivery*, 7(4),1912-9, 1992.
- [5] Sidhu TS, Sachdev MS, Wood HC and Nagpal M, "Design, Implementation and Testing of a Microprocessor-Based High-Speed Relay for Detecting Transformer Winding Faults," *IEEE Trans Power Delivery*, 7(1),108-17, 1992.